

Anharmonic effects in thermoelectric and 2D materials

Unai Aseguinolaza Aguirreche

Supervised by Aitor Bergara and Ion Errea

September 17, 2020

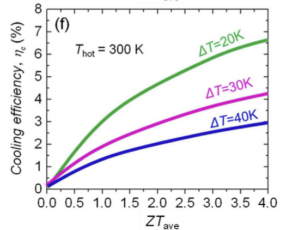
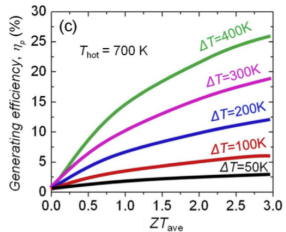
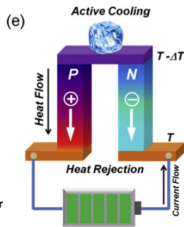
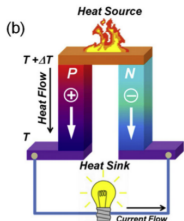


Outline

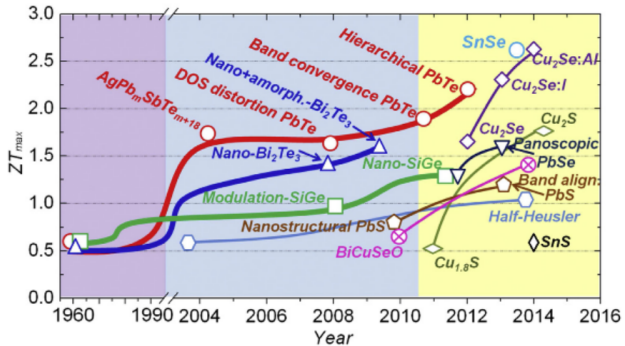
- Introduction
- Theoretical framework
- Part 1: Thermoelectric monochalcogenides
- Part 2: 2D materials
- Conclusions

Introduction

$$ZT = \frac{S^2 \sigma T}{\kappa}, \quad S = -\frac{\Delta V}{\Delta T}$$



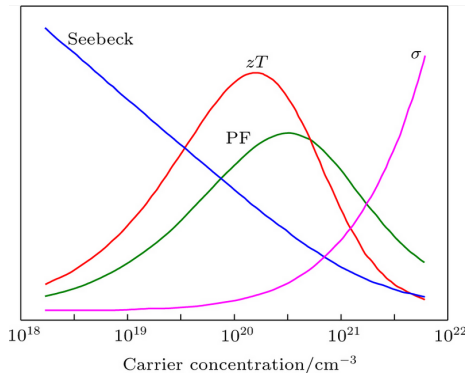
Introduction



- ZT_{max} low and in narrow temperature ranges
- Very limited technological applications.

X. Zhang, L-D. Zhao / Journal of Materomics 1 (2015) 92-105

Introduction



- The physical magnitudes that define ZT are correlated
- How to overcome:
 - Doping + nanostructuring
 - Proximity to phase transitions
 - ...

Ultralow thermal conductivity and high thermoelectric figure of merit in SnSe crystals

Li-Dong Zhao¹, Shih-Han Lo², Yongsheng Zhang², Hui Sun³, Gangjian Tan¹, Ctarad Uher³, C. Wolverton², Vinayak P. Dravid² & Mercouri G. Kanatzidis¹

The thermoelectric effect enables direct and reversible conversion between thermal and electrical energy, and provides a viable route for power generation from waste heat. The efficiency of thermoelectric materials is dictated by the dimensionless figure of merit, ZT (where Z is the figure of merit and T is absolute temperature), which governs the Carnot efficiency for heat conversion. Enhancements above the generally high threshold value of 2.5 have important implications for commercial deployment^{1–3}, especially for compounds free of Pb and Te. Here we report an unprecedented ZT of 2.6 ± 0.3 at 923 K, realized in SnSe single crystals measured along the b axis of the room-temperature orthorhombic unit cell. This material also shows a high ZT of 2.3 ± 0.3 along the c axis but a significantly reduced ZT of 0.8 ± 0.2 along the a axis. We attribute the remarkably high ZT along the b axis to the intrinsically ultralow lattice thermal conductivity in SnSe. The layered structure of SnSe derives from a distorted rock-salt structure, and features anomalously high Grüneisen parameters, which reflect the anharmonic and anisotropic bonding. We attribute the exceptionally low lattice thermal conductivity ($0.23 \pm 0.03 \text{ W m}^{-1} \text{ K}^{-1}$ at 973 K) in SnSe to the anharmonicity. These findings highlight alternative strategies to nanostructuring for achieving high thermoelectric performance.

power factor (along the b axis), but, even more surprisingly, we observe that the thermal conductivity of SnSe is intrinsically ultralow ($<0.25 \text{ W m}^{-1} \text{ K}^{-1}$ at $>800 \text{ K}$), resulting in $ZT = 2.62$ at 923 K along the b axis and 2.3 along the c axis; these represent the highest ZT values reported so far for any thermoelectric system. Along the a direction, however, ZT is significantly lower, ~ 0.8 . Here, it should be noted that SnSe along the b axis shows a room-temperature $ZT = 0.12$, which is comparable to the room-temperature value of 0.15 reported earlier¹⁹. SnSe, however, reveals high ZT values near and above the transition temperature of 750 K at which the structure converts from $Pnma$ to $Cmcm$ ^{20–22}. Such ultrahigh ZT along two principal directions and the observed crystallographic and ZT anisotropy prompted us to investigate the scientific underpinning of these intriguing results.

SnSe adopts a layered orthorhombic crystal structure at room temperature, which can be derived from a three-dimensional distortion of the NaCl structure. The perspective views of the room-temperature SnSe crystal structure along the a , b and c axial directions are shown in Fig. 1a–d. There are two-atom-thick SnSe slabs (along the b – c plane) with strong Sn–Se bonding within the plane of the slabs, which are then linked with weaker Sn–Se bonding along the a direction²⁰. The structure contains highly distorted SnSe_2 coordination polyhedra, which have

- The best thermoelectric material so far: Intrinsic semiconductor with low lattice thermal conductivity ($\kappa = \kappa_{el} + \kappa_l$)

Introduction

The periodic table shows the Chalcogenides (group 16) highlighted in red. The elements include Sulfur (S), Selenium (Se), and Tellurium (Te). Other elements shown include Hydrogen (H), Helium (He), Lithium (Li), Beryllium (Be), Sodium (Na), Magnesium (Mg), Potassium (K), Calcium (Ca), Scandium (Sc), Titanium (Ti), Vanadium (V), Chromium (Cr), Manganese (Mn), Iron (Fe), Cobalt (Co), Nickel (Ni), Copper (Cu), Zinc (Zn), Gallium (Ga), Germanium (Ge), Arsenic (As), and Antimony (Sb).

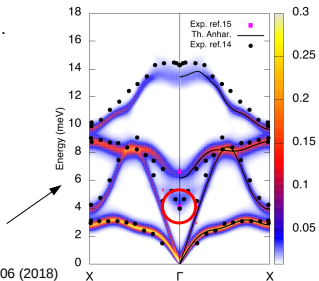
Chalcogenides

Monochalcogenides: PbTe, SnTe, GeTe, SnS...

Low lattice thermal conductivity

They show strongly anharmonic features:

- Lattice instabilities in the harmonic phonons
- Ferroelectric transitions
- Incipient ferroelectricity
- Special features in the phonon spectral function



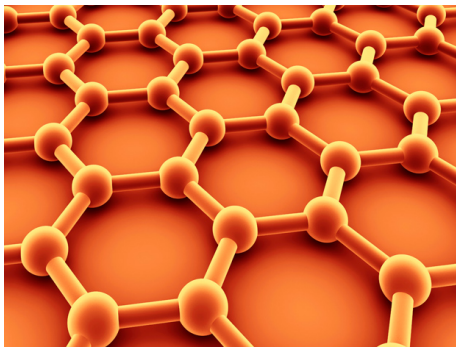
G. A. Ribeiro et al. Physical Review B 97, 014306 (2018)

- Anharmonic effects are the key

Introduction

Applications of 2D materials:

- 2D thermoelectrics (Advanced materials 19.8 (2007): 1043-1053)
- Low dimensional heat dissipators (The Journal of Physical Chemistry C 122.5 (2018): 2641-2647)



- Harmonic approximation does not work (Acoustic phonons)

Theoretical framework

- Ionic Hamiltonian

$$H = T + V(\mathbf{R})$$

where $\mathbf{R} = \mathbf{R}_0 + \mathbf{u}$.

- Assuming that $V(\mathbf{R})$ is well reproduced by a quadratic potential in the range of \mathbf{u} , Taylor expand the potential

$$V(\mathbf{R}) \simeq V(\mathbf{R}_0) + \frac{1}{2} \sum_{ab} \phi_{ab} u_a u_b + O(u^3)$$

where $\phi_{ab} = \partial^2 V / \partial u_a \partial u_b|_0$.

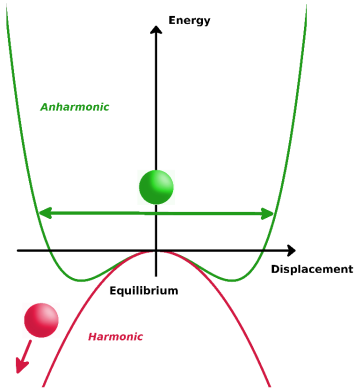
$$V^{harm}(\mathbf{R}) = V(\mathbf{R}_0) + \frac{1}{2} \sum_{ab} \phi_{ab} u_a u_b$$

- This Hamiltonian (Harmonic Hamiltonian) can be solved exactly.
- It provides well defined phonon quasiparticles

$$\sum_b \phi_{ab} \epsilon_\mu^b = M \omega_\mu^2 \epsilon_\mu^a$$

Theoretical framework

- Harmonic approximation:
 - It does not work in monochalcogenides because they show harmonic instabilities.
- Perturbative approaches are not an option.
 - They are built on top of the harmonic theory.
- We apply a variational non-perturbative approach with anharmonic terms to infinite order: Stochastic self-consistent harmonic approximation (SSCHA)



Theoretical framework

- SCHA is a method for approximating the vibrational free energy of a crystal.

$$F_H = \text{tr}(\rho_H H) + \frac{1}{k_B T} \text{tr}(\rho_H \ln \rho_H)$$

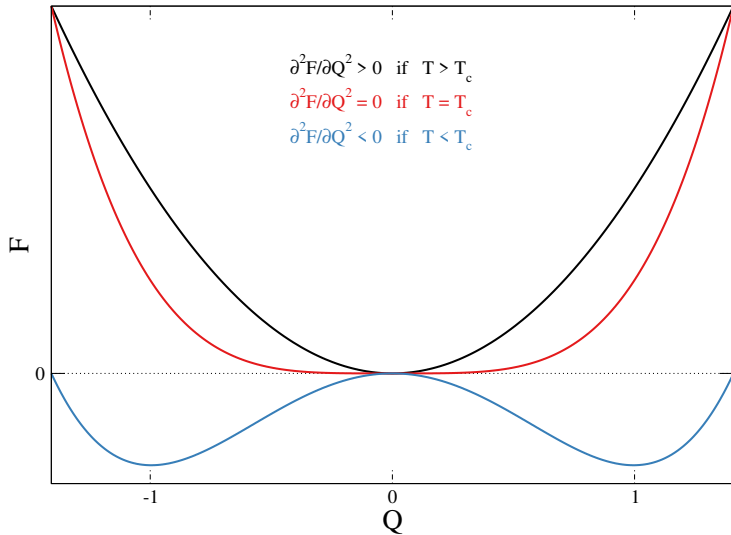
$$\mathcal{F}_H[\mathcal{H}] = \text{tr}(\rho_{\mathcal{H}} H) + \frac{1}{k_B T} \text{tr}(\rho_{\mathcal{H}} \ln \rho_{\mathcal{H}}) = F_{\mathcal{H}} + \langle V - \mathcal{V} \rangle_{\rho_{\mathcal{H}}}$$

$$F_H \leq \mathcal{F}_H[\mathcal{H}]$$

- We take a harmonic trial density matrix $\rho_{\mathcal{H}} \equiv \rho_{\mathcal{H}}(\Phi, \mathcal{R})$. Variables Φ (SCHA/auxiliary phonons) and \mathcal{R} atomic centroids.
- The SCHA provides the harmonic density matrix that minimizes the free energy.

Theoretical framework

- Landau Theory of second-order phase transitions



Theoretical framework

- The free energy is a well defined quantity within the SCHA.
- For a given temperature, experimentally measured phonon frequencies will be centered in the phonon frequencies defined by $\partial^2 \mathcal{F} / \partial \mathbf{R}^2$.

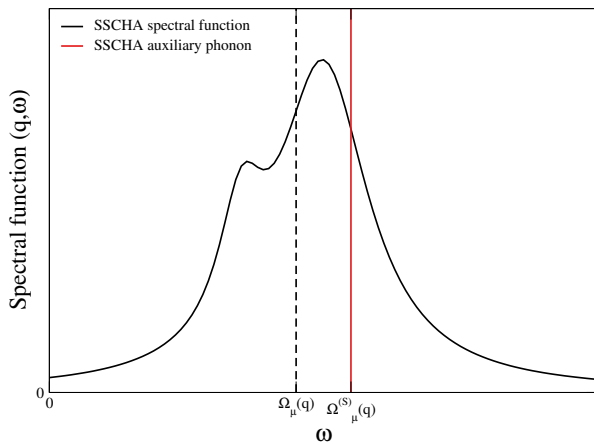
$$\frac{\partial^2 \mathcal{F}}{\partial \mathbf{R} \partial \mathbf{R}} = \Phi + \overset{(3)}{\Phi} \Lambda [1 - \overset{(4)}{\Phi} \Lambda]^{-1} \overset{(3)}{\Phi}$$

- $\overset{(3)}{\Phi} = \left\langle \frac{\partial^3 V}{\partial \mathbf{R}^3} \right\rangle_{\rho_H}$, $\overset{(4)}{\Phi} = \left\langle \frac{\partial^4 V}{\partial \mathbf{R}^4} \right\rangle_{\rho_H}$, and $\Lambda \equiv \Lambda(\Phi, T)$.
- They are different to the perturbative ones $[\partial^3 V / \partial \mathbf{R}^3]_0$, $[\partial^4 V / \partial \mathbf{R}^4]_0$

Theoretical framework

- The static theory can be expanded by a dynamical ansatz.

$$\sigma(\mathbf{q}, \omega) = \frac{1}{\pi} \times \sum_{\mu} \frac{-\omega Im\Pi_{\mu}(\mathbf{q}, \omega)}{(\omega^2 - \Omega_{\mu}^{(S)2}(\mathbf{q}) - Re\Pi_{\mu}(\mathbf{q}, \omega))^2 + (Im\Pi_{\mu}(\mathbf{q}, \omega))^2}$$



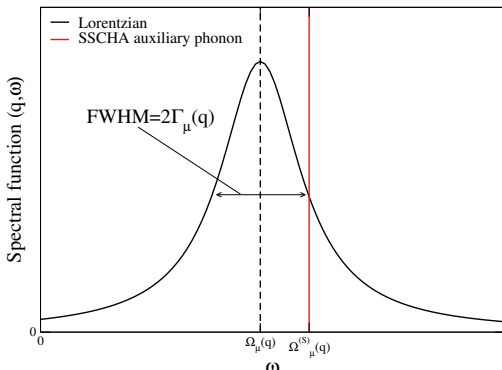
Theoretical framework

$$\mathcal{Z}_\mu(\mathbf{q}, \omega) = \sqrt{\Omega_\mu^{(S)2}(\mathbf{q}) + \Pi_\mu(\mathbf{q}, \omega + i0^+)}$$

$$\Omega_\mu(\mathbf{q}) = \text{Re} \mathcal{Z}_\mu(\mathbf{q}, \Omega_\mu^{(S)}(\mathbf{q})),$$

$$\Omega_\mu^{(F)}(\mathbf{q}) = \text{Re} \mathcal{Z}_\mu(\mathbf{q}, 0) = \partial^2 \mathcal{F} / \partial \mathcal{R}^2,$$

$$\Gamma_\mu(\mathbf{q}) = -\text{Im} \mathcal{Z}_\mu(\mathbf{q}, \Omega_\mu^{(S)}(\mathbf{q}))$$



Theoretical framework

- The Lorentzian definition of phonons provides a straightforward way of calculating the lattice thermal conductivity

$$\kappa_I = \frac{1}{N_{\mathbf{q}} \Omega_{cell} k_B T^2} \sum_{\mathbf{q}\mu} v_\mu(\mathbf{q})^2 \omega_\mu(\mathbf{q})^2 n_B(\omega_\mu(\mathbf{q})) [n_B(\omega_\mu(\mathbf{q})) + 1] \tau_\mu(\mathbf{q}).$$

SSCHA stress tensor (different to the BO stress tensor):

$$P_{\alpha\beta}^{SSCHA}(\mathcal{R}, \{\mathbf{a}_i\}) = -\frac{1}{\Omega} \left. \frac{\partial \mathcal{F}_H[\mathcal{R}, \{\mathbf{a}_i\}]}{\partial \epsilon_{\alpha\beta}} \right|_{\epsilon=0}$$

SSCHA computation method:

- Supercell are generated with the harmonic density matrix and random numbers
- The forces in supercell are used to compute the gradient of \mathcal{F} and interatomic force-constants (forces at any theoretical level)

Theoretical framework

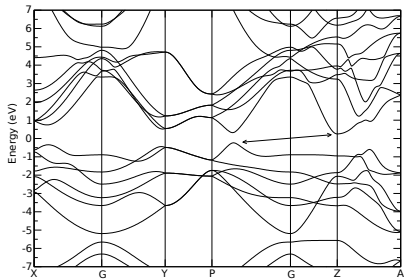
SSCHA summary:

- Anharmonic free energy
- Phase transition temperature
- Anharmonic phonons
- Anharmonic stress tensor
- Lattice thermal conductivity

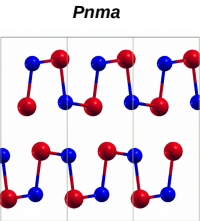
Part One:

- Bulk SnSe
- Bulk SnS
- Monolayer SnSe

SnSe

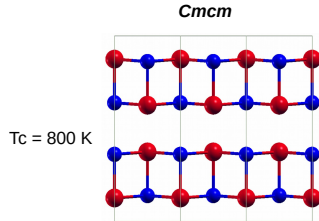


Low T, low symmetry



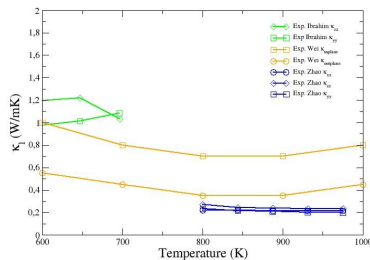
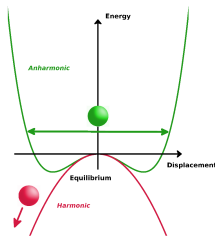
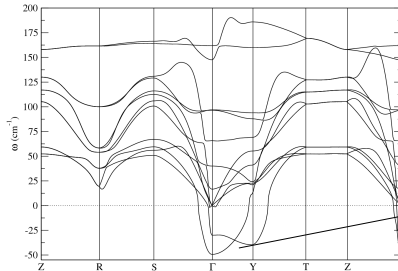
- Anisotropic crystal structure
- Narrow gap semiconductor
- Structural phase transition

High T, high symmetry



$T_c = 800 \text{ K}$

SnSe



- Lattice instabilities in the harmonic approximation
In the high temperature phase
- Ultralow thermal conductivity
- Experimental discrepancy
 - Value
 - Anisotropy

Ibrahim et al. Appl. Phys. Lett. 110, 032103 (2017), Zhao et al. Nature 508, 373 (2014),

Wei et al. ACS Omega 4, 5442-5450 (2019)

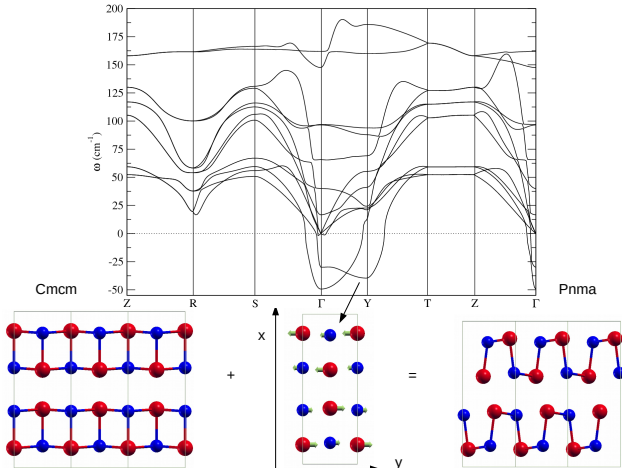
Unai Aseguinolaza Aguirreche

September 17, 2020

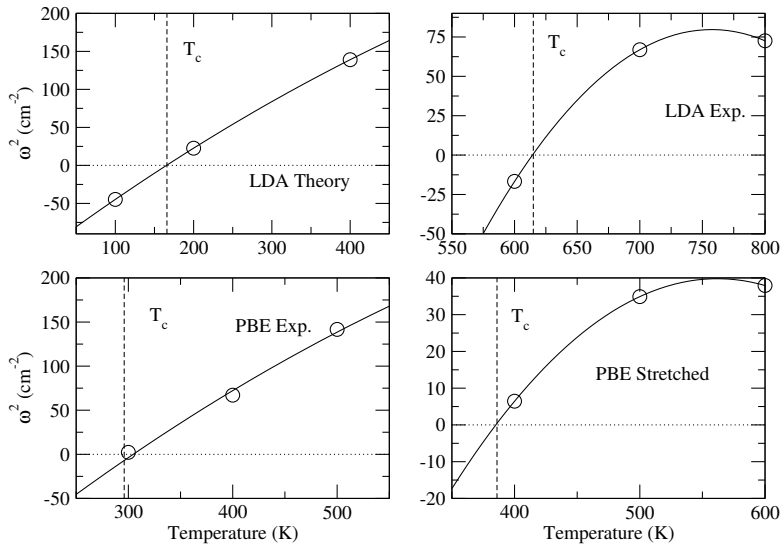
20 / 56

SnSe

$$\frac{\partial^2 F}{\partial Q^2} \propto \omega_{Y_1}^2(T), \quad \frac{\partial^2 F}{\partial \mathcal{R} \partial \mathcal{R}} = \Phi + \overset{(3)}{\Phi} W \overset{(3)}{\Phi}, \quad \overset{(3)}{\Phi} = \left\langle \frac{\partial^3 V}{\partial \mathcal{R}^3} \right\rangle$$

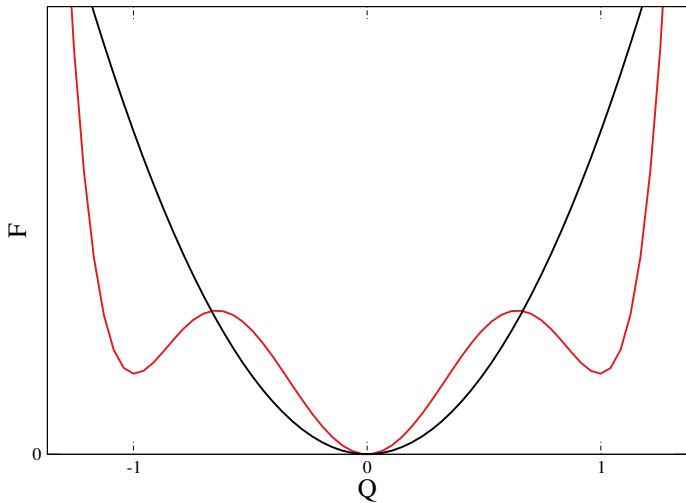


SnSe



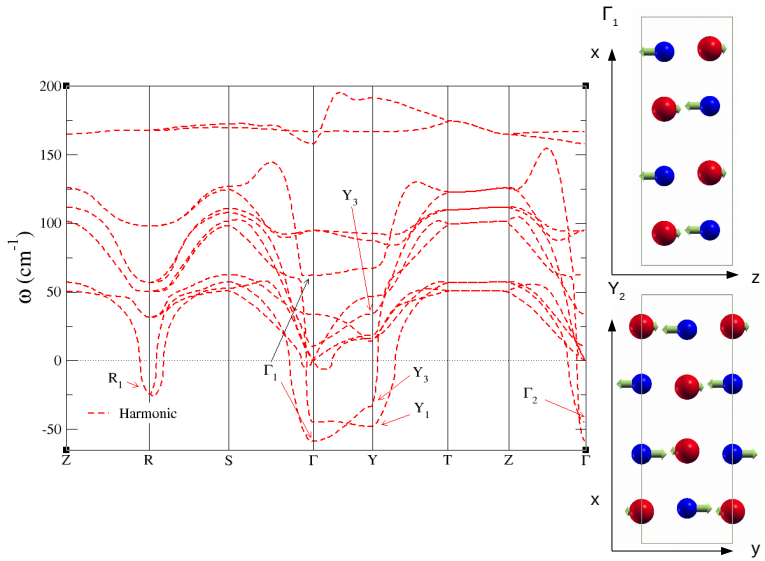
- We use LDA/Exp for the computations

SnSe

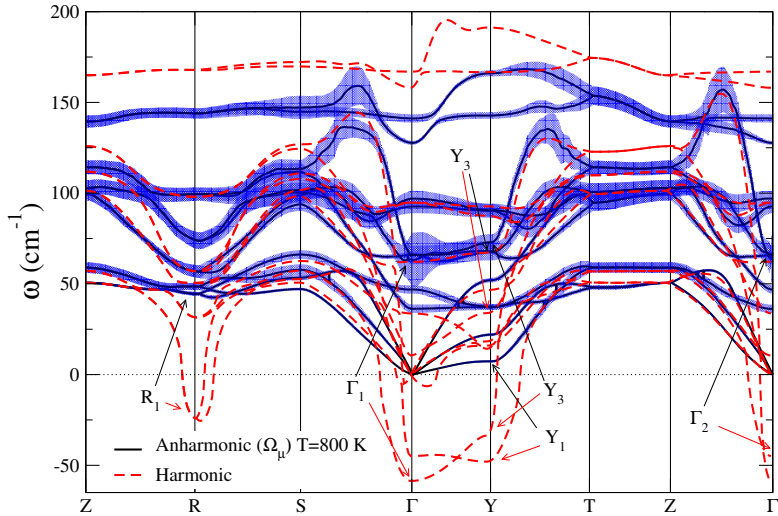


- We discard the first-order phase transition.

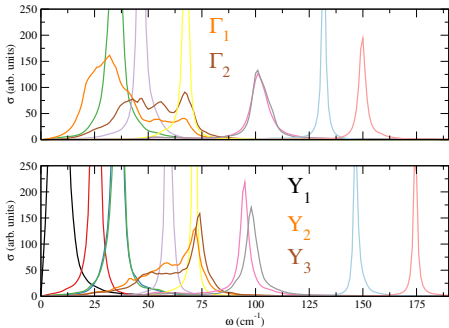
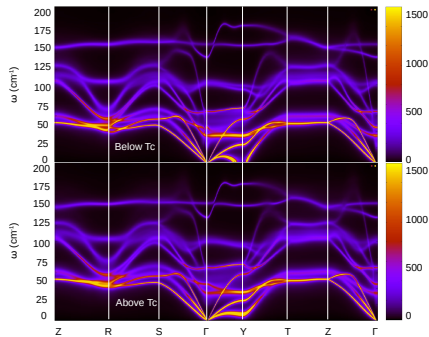
SnSe



SnSe



SnSe

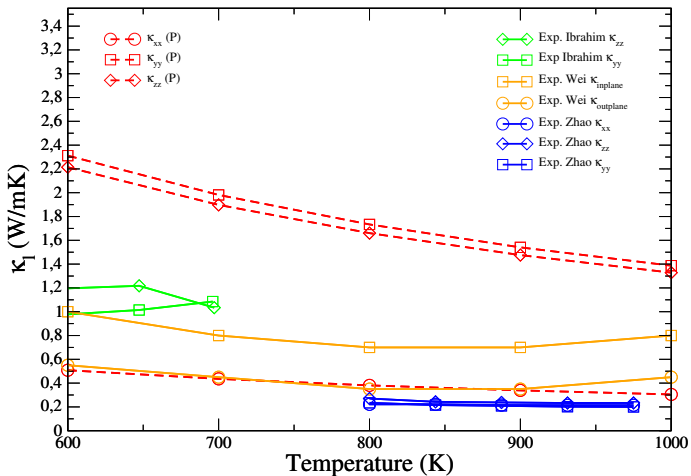


- The phase transition is measurable in INS experiments.
- There are modes that strongly deviate from the Lorentzian limit.

U. Aseginolaza et al. PRL 122, 075901 (2019)

SnSe

- We use the SSCHA auxiliary phonons at 800 K



L.D. Zhao et al. Nature 508, 373 (2014), Ibrahim et al. Appl. Phys. Lett. 110, 032103 (2017),

U. Aseginolaza et al. PRL 122, 075901 (2019)

- Perturbative

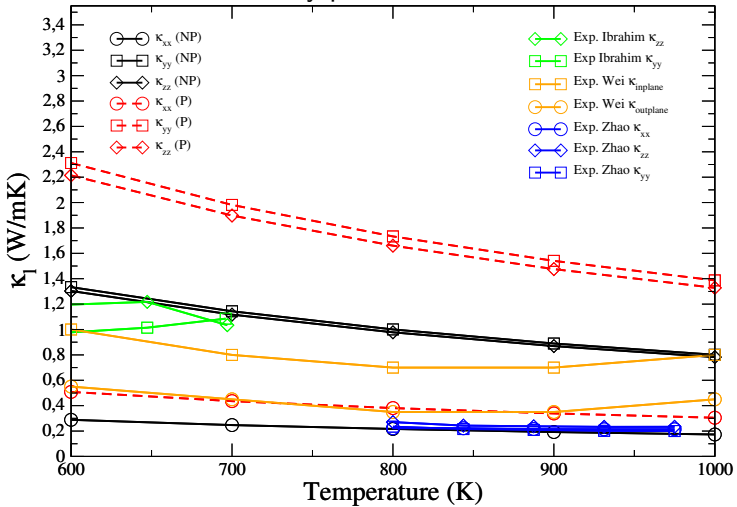
$$\left[\frac{\partial^3 V}{\partial \mathbf{R}^3} \right]_0$$

- Non-perturbative

$$\left\langle \frac{\partial^3 V}{\partial \mathbf{R}^3} \right\rangle_{\rho_{\mathcal{H}}}$$

SnSe

- We use the SSCHA auxiliary phonons at 800 K

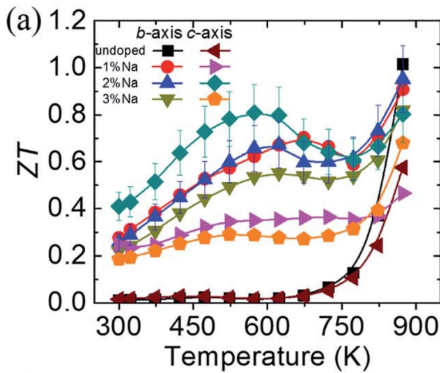
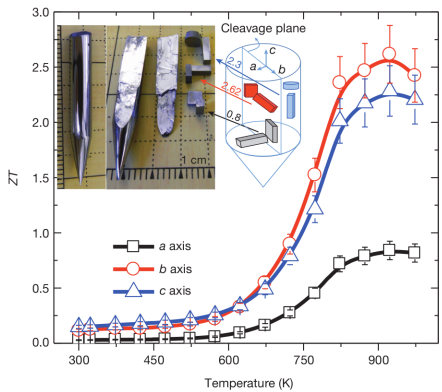


L.D. Zhao et al. Nature 508, 373 (2014), Ibrahim et al. Appl. Phys. Lett. 110, 032103 (2017),

U. Aseginolaza et al. PRL 122, 075901 (2019)

SnSe and SnS

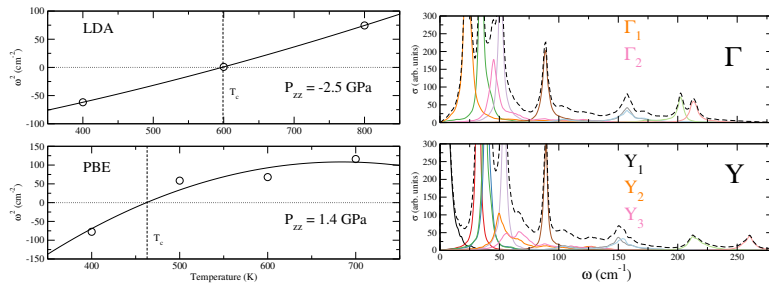
Left: SnSe, Right: SnS



- They look very similar thermoelectric materials.

SnSe and SnS

What about SnS?



- Second-order phase transition, best agreement with LDA/Exp
- Strong anharmonic renormalization
- Non-Lorentzian phonons

SnSe and SnS

$$ZT = \frac{P_F T}{\kappa}, \quad P_F = S^2 \sigma$$

$$\sigma(T, \mu) = e^2 \int_{-\infty}^{\infty} d\varepsilon \left[-\frac{\partial f(T, \mu, \varepsilon)}{\partial \epsilon} \right] \Sigma(\varepsilon),$$

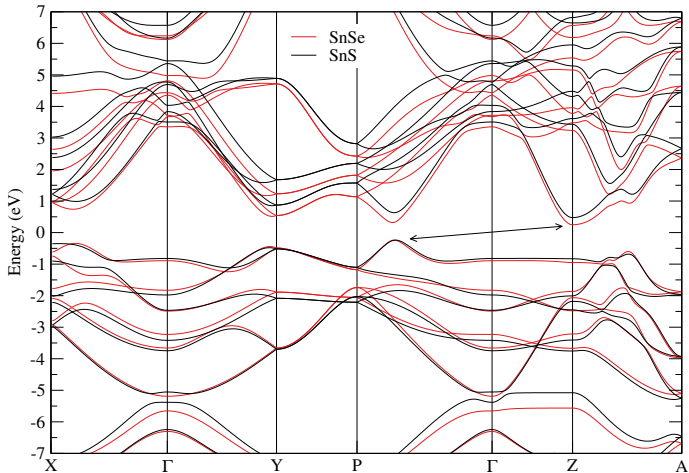
$$S(T, \mu) = \frac{e}{T \sigma(T, \mu)} \int_{-\infty}^{\infty} d\varepsilon \left[-\frac{\partial f(T, \mu, \varepsilon)}{\partial \epsilon} \right] \Sigma(\varepsilon)(\varepsilon - \mu),$$

$$\Sigma(\varepsilon) = \frac{1}{\Omega N_{\mathbf{k}}} \sum_{n\mathbf{k}} \tau_{n\mathbf{k}}^e |\mathbf{v}_{n\mathbf{k}}|^2 \delta(\varepsilon - \varepsilon_{n\mathbf{k}}),$$

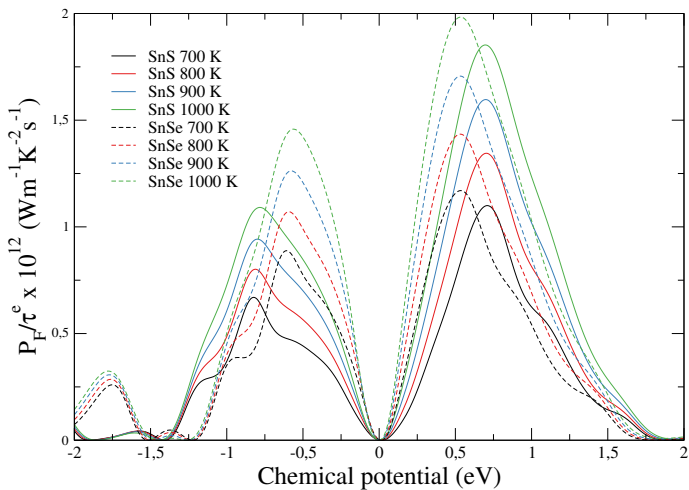
- We use the Boltztrap software package

G. K. Madsen et al. Computer Physics Communications 175, 67 (2006)

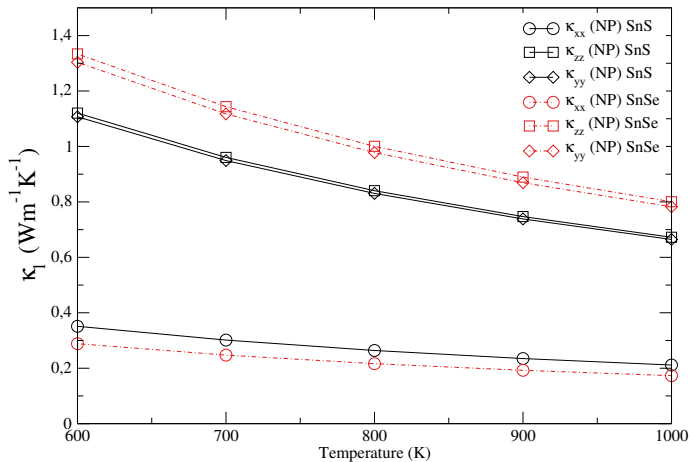
SnSe and SnS



SnSe and SnS



SnSe and SnS



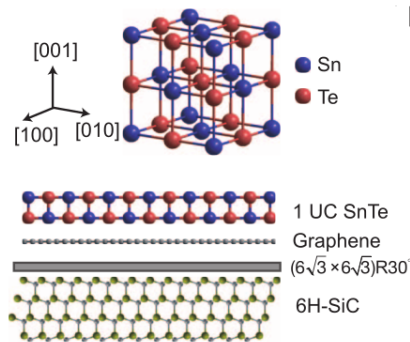
SnSe and SnS: Conclusions

- Second-order phase transitions
- Strongly anharmonic phonon spectra
- Ultralow anisotropic lattice thermal conductivity, important non-perturbative effects
- Both materials show similar electronic and vibrational properties

Monolayer SnSe

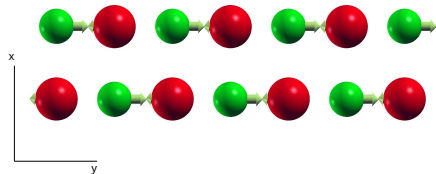
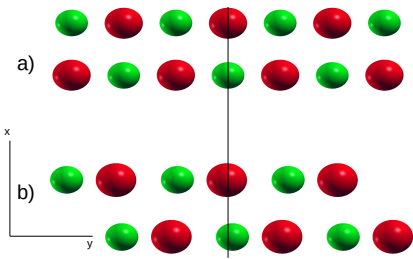
Two reasons to study monolayer SnSe:

- Theoretical calculations claim it could be an efficient thermoelectric material
- It could be an atomically thick ferroelectric material



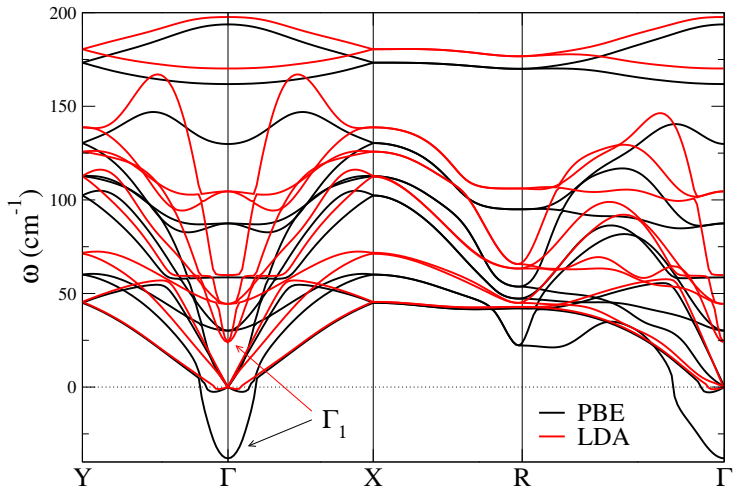
This is the case in SnTe (Kai Chang et al. Science 353, 6296 (2016))

Monolayer SnSe



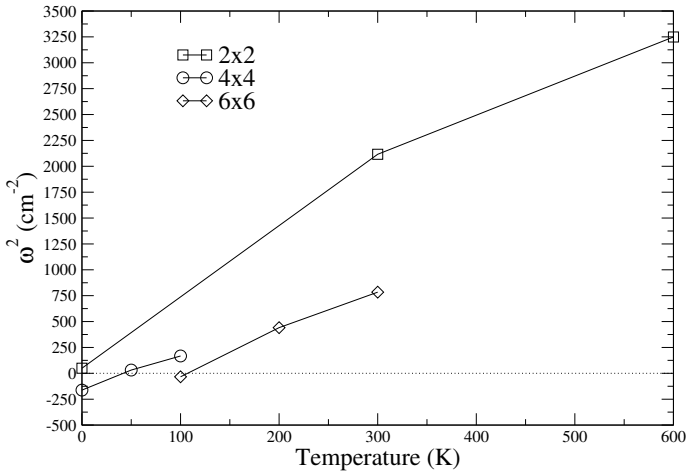
- This is the ferroelectric transition (in the monolayer)
- a) High symmetry phase ($Q = 0$) $Pnmm$
- b) Low symmetry phase ($Q \neq 0$) $Pnm2_1$
- Atomic displacements correspond to a phonon at the Γ point

Monolayer SnSe



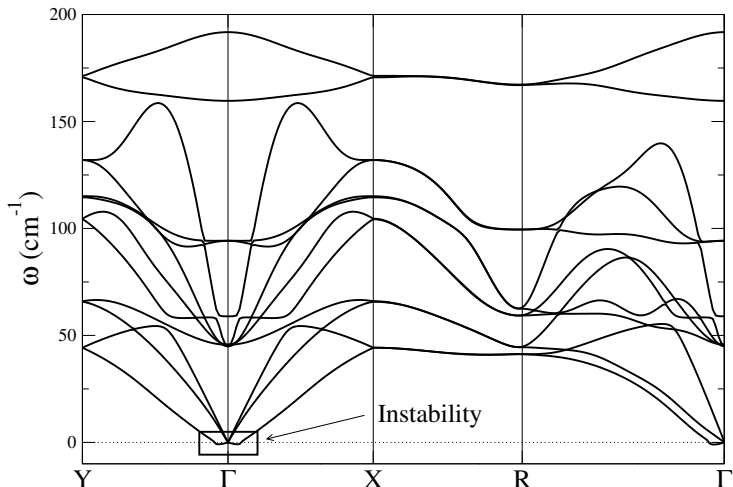
- The calculations are done with theoretical lattice parameters
- We perform the SSCHA calculation only within PBE

Monolayer SnSe



- Good agreement with other theoretical calculations
- Strong supercell size dependence on T_c

Monolayer SnSe



- Tiny instabilities do not allow us to compute κ_I

Monolayer SnSe

Conclusions:

- We theoretically predict the ferroelectric phase transition
- Unstable Fourier interpolation of the SSCHA auxiliary phonons
 - Motivation for the study of the anharmonic effects on the lowest energy acoustic branch of 2D materials.

Part two:

- 2D materials: Graphene

Graphene

PHYSICAL REVIEW

VOLUME 176, NUMBER 1

5 DECEMBER 1968

Crystalline Order in Two Dimensions*

N. D. Mermin[†]

Laboratory of Atomic and Solid State Physics, Cornell University, Ithaca, New York

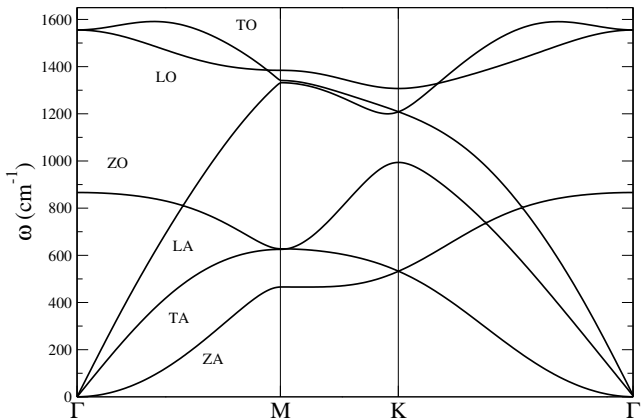
(Received 1 July 1968)

If N classical particles in two dimensions interacting through a pair potential $\Phi(\vec{r})$ are in equilibrium in a parallelogram box, it is proved that every $k \neq 0$ Fourier component of the density must vanish in the thermodynamic limit, provided that $\Phi(\vec{r}) - \lambda r^2 |\nabla^2 \Phi(\vec{r})|$ is integrable at $r = \infty$ and positive and nonintegrable at $r = 0$, both for $\lambda = 0$ and for some positive λ .

This result excludes conventional crystalline long-range order in two dimensions for power-law potentials of the Lennard-Jones type, but is inconclusive for hard-core potentials. The corresponding analysis for the quantum case is outlined. Similar results hold in one dimension.

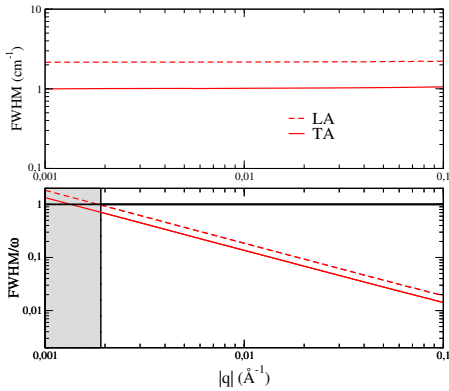
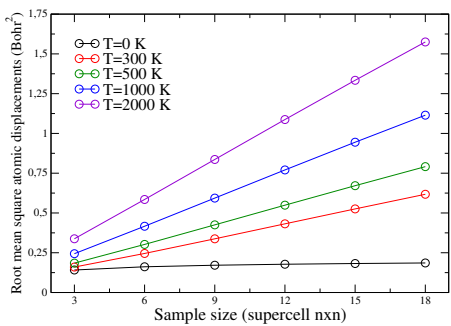
- The existence of 2D materials was not believed to be possible.
- Nowadays there is a whole branch of science exploiting their applications.

Graphene



- $\omega_{ZA}(|\mathbf{q}|) = \alpha|\mathbf{q}| + \beta|\mathbf{q}|^2 + \dots$
- Rotational invariance (RI) together with the 2D character of ϕ_{ab} makes the harmonic dispersion of mode ZA quadratic ($\alpha = 0$).

Graphene



- $\langle u^2 \rangle$ diverges for finite temperatures.
- Finite linewidths of LA/TA modes at decreasing momenta.
Quasiparticle picture and sound propagation lost in graphene.
- Both properties arise due to the quadratic ZA modes.

Graphene

The problems we have mentioned are long standing problems:

- Perturbation theory predicts a linear dispersion
- The bending rigidity $\kappa(q) \propto \omega_{ZA}/q^2$ diverges

What phonons do we expect from a theoretical point of view?

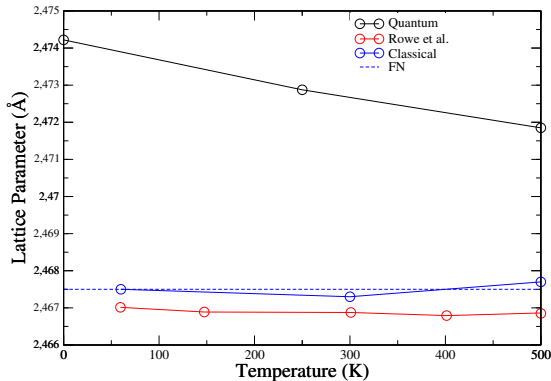
- Phonons defined from the free energy \mathcal{F} should be quadratic as the ones defined from the harmonic potential V . Both have the same symmetries.

What have we done?

- ① Perform SCHA in an atomistic model using an empirical machine learning potential trained with DFT.

Graphene

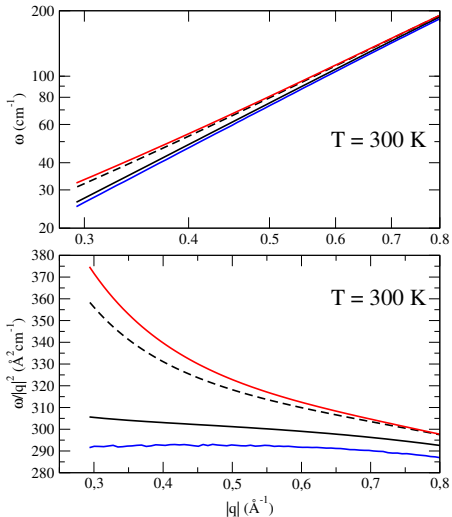
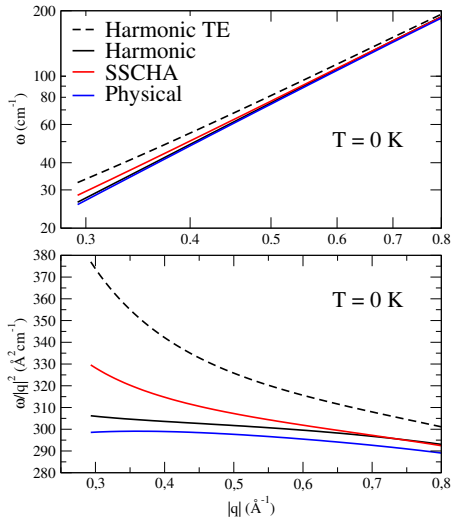
$$P_{\alpha\beta}^{SSCHA}(\mathcal{R}, \{\mathbf{a}_i\}) = -\frac{1}{\Omega} \frac{\partial \mathcal{F}_H[\mathcal{R}, \{\mathbf{a}_i\}]}{\partial \epsilon_{\alpha\beta}} \Big|_{\epsilon=0}$$



- Strain break rotational invariance
- Strain linearizes the ZA dispersion

Graphene

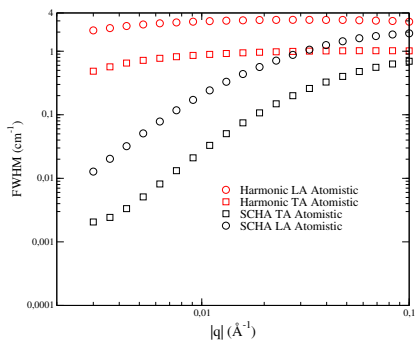
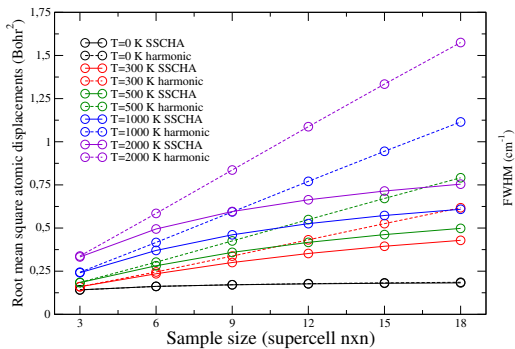
ZA phonons



- The bending rigidity does not diverge

Graphene

- We calculate $\langle u^2 \rangle$ using the density matrix given by the SCHA
- We calculate the FWHM using the SCHA phonons for the three phonon scattering phase space



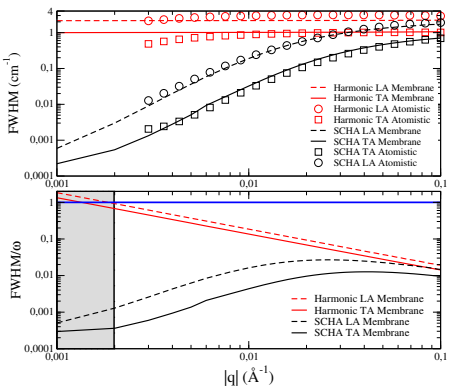
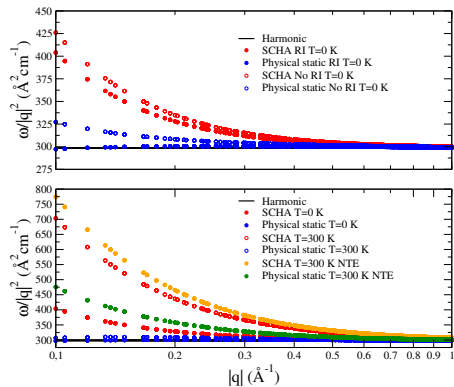
- Quasiparticle picture and sound propagation recovered

Graphene

$$V = \frac{1}{2} \int_{\Omega} d^2x [\kappa (\partial^2 h)^2 + C^{ijkl} \partial_i u_j \partial_k u_l + C^{ijkl} \partial_i u_j \partial_k h \partial_l h \\ + \frac{C^{ijkl}}{4} \partial_i h \partial_j h \partial_k h \partial_l h + \frac{C^{ijkl}}{2} \partial_i \mathbf{u} \cdot \partial_j \mathbf{u} \partial_k h \partial_l h + C^{ijkl} \partial_i u_j \partial_k \mathbf{u} \cdot \partial_l \mathbf{u} \\ + \frac{C^{ijkl}}{4} \partial_i \mathbf{u} \cdot \partial_j \mathbf{u} \partial_k \mathbf{u} \cdot \partial_l \mathbf{u}]$$

- This is an universal potential for all 2D materials
- $u_i(x)$ where $i = x, y$ and $h(x)$ are the in-plane and out-of-plane displacement fields.
- $C^{ijkl} = \lambda \delta^{ij} \delta^{kl} + \mu (\delta^{ik} \delta^{jl} + \delta^{il} \delta^{jk})$ where λ, μ are the Lame coefficients.
- κ is the bending rigidity and Ω the area of the membrane.
- $\partial_i u_j \rightarrow \partial_i u_j + \delta^{ij} \delta a$ where $\delta a = (a - a_0)/a_0$.

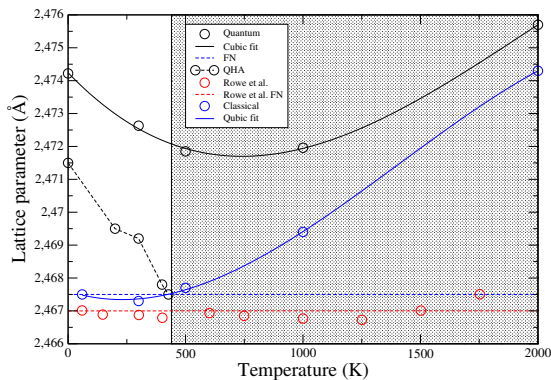
Graphene



- SCHA phonons are linear
- Physical phonons are quadratic. Bending rigidity does not diverge
- LA/TA linewidths decay and sound can propagate

Graphene

What happens at higher temperatures?



- First of all: QH does not work
- At high temperatures MD and SSCHA do not match
- Corrugated phase at high temperatures? (FUTURE RESEARCH)

Graphene

Conclusions:

- ① We perform simulations in strain less membranes by using the SSCHA stress tensor
- ② Anharmonicity linearises the auxiliary phonons
- ③ Divergencies removed, quasiparticle picture recovered
- ④ Physical phonons have a quadratic dispersion as expected for RI membranes
- ⑤ Universal features for all 2D materials

General conclusions

- Anharmonicity crucial for understanding phase stabilities
- Efficient thermoelectrics show strongly anharmonic non-Lorentzian phonons
- Non-perturbative force-constants are important in efficient thermoelectrics
- Quasiparticle picture of phonons and sound propagation recovered by anharmonicity
- The physical phonons of 2D materials are quadratic, as expected by symmetry

Acknowledgements

Supervisors:

- Ion Errea and Aitor Bergara

All the group members:

- Miguel Borinaga
- Raffaello Bianco

Collaborators:

- Lorenzo Monacelli
- Francesco Mauri
- Matteo Calandra
- Lorenzo Paulatto